

Formation and decay of Hg₂ excimers in Hg-Ar mixtures*

I. N. Siara and L. Krause

Department of Physics, University of Windsor, Windsor, Ontario, Canada

(Received 3 February 1975)

The formation and decay of Hg₂ molecules in their ³1_u and ³0_u⁻ states, produced in Hg-Ar mixtures irradiated with 2537-Å Hg resonance radiation, has been investigated by the method of delayed coincidences. The mixtures which consisted of Hg vapor at a pressure of about 1 Torr and Ar at pressures of 45–720 Torr and which were contained in a quartz fluorescence cell, were excited with pulses of light, and the decay spectra of the 3350- and 4850-Å molecular fluorescent bands were studied in relation to Ar pressure. Analysis of the decays indicates that the effective cross sections for ³1_u ↔ ³0_u⁻ mixing, induced in Hg₂-Ar collisions are of the same order as the Hg₂-N₂ mixing cross sections, leading to the conclusion that the 4850-Å band is emitted mainly by ³0_u⁻ molecules in high vibrational states.

I. INTRODUCTION

Phaneuf, Skonieczny, and Krause¹ have recently proposed a mechanism for the formation and decay of excited Hg₂ molecules in Hg-N₂ mixtures. Based on Mrozowski's early postulates,^{2,3} their model assigns the 3350-Å ultraviolet and the 4850-Å green bands to the ¹Σ_g⁺ - ³1_u and ¹Σ_g⁺ - ³0_u⁻ transitions, respectively, in the Hg₂ excimer molecules. The mechanism which is also consistent with the findings of other investigators,^{4,5} predicts that the ³1_u excimer state is formed first in a triple collision of an Hg(³P₀) metastable atom, a ground-state Hg(¹S₀) atom and a N₂ molecule. Because of very efficient ³1_u ↔ ³0_u⁻ mixing, some of the ³1_u molecules are transferred to the metastable ³0_u⁻ state which has a radiative lifetime of about 21 msec.⁶ Both ³0_u⁻ and ³1_u molecules are assumed to decay spontaneously to the dissociative ¹Σ_g⁺ ground state, the latter with a decay constant comparable to that of the atomic 6³P₁ resonance state.³

In order to obtain further information about the ³1_u ↔ ³0_u⁻ collisional mixing process, we have decided to study the formation and decay of the Hg₂ excimers in Hg-Ar mixtures using, as before,¹ the method of delayed coincidences. Because the high efficiency of the mixing observed in a Hg₂-N₂ system might be due to the participation of N₂ vibrational and rotational modes, it was decided to use the argon atom as collision partner to eliminate the effect of the internal molecular degrees of freedom on the mixing process. The relatively large mass of the Ar atom is also useful because it inhibits the diffusion of metastable species out of the region of observation⁷ and to the cell walls,⁸ and reduces the errors caused by the diffusion, in the measured decay rates.

The relevant potential curves for the Hg₂ molecules as proposed by Mrozowski,³ are shown in Fig. 1. The diagram also indicates the radiative

and collisional processes involved in the population and decay of the various atomic and molecular states. If it is assumed that collisional quenching of excited atoms and molecules to their ground states is negligible, the following rate equations may be written for the populations *n_i* of the various atomic and molecular states:

$$\dot{n}_1 = Z_{21}n_2 - (\Gamma_1 + Z_{12} + Z_{13})n_1, \quad (1)$$

$$\dot{n}_2 = Z_{12}n_1 - (\Gamma_2 + Z_{21})n_2, \quad (2)$$

$$\dot{n}_3 = Z_{13}n_1 + Z_{43}n_4 - (\Gamma_3 + Z_{34})n_3, \quad (3)$$

$$\dot{n}_4 = Z_{34}n_3 - (\Gamma_4 + Z_{43})n_4, \quad (4)$$

where Γ_i is the spontaneous decay constant for state *i* and $Z_{ij} = NQ_{ij}v_r$ represents the frequency of collisions per excited atom or molecule in state *i*, resulting in its transfer to state *j*; Q_{ij} is the total average cross section for the collisional transfer, v_r is the average relative speed of the collision partners, *N* is the density of argon atoms and *i, j* = 1, 2, 3, 4, where the subscripts 1, 2, 3, 4 refer to the states 6³P₀, 6³P₁, ³1_u, and ³0_u⁻, respectively. Equations (1) and (2) yield the following two second-order homogeneous differential equations:

$$\ddot{n}_1 + (R_1 + R_2)\dot{n}_1 + (R_1R_2 - Z_{12}Z_{21})n_1 = 0, \quad (5)$$

$$\ddot{n}_2 + (R_1 + R_2)\dot{n}_2 + (R_1R_2 - Z_{12}Z_{21})n_2 = 0, \quad (6)$$

where $R_1 \equiv \Gamma_1 + Z_{12} + Z_{13}$ and $R_2 \equiv \Gamma_2 + Z_{21}$. The solutions of Eqs. (5) and (6) are

$$n_1 = Ae^{-\Gamma'_m t} + Be^{-\Gamma''_m t}, \quad (7)$$

$$n_2 = A'e^{-\Gamma'_m t} + B'e^{-\Gamma''_m t}, \quad (8)$$

where

$$\Gamma_m = \frac{1}{2}(R_1 + R_2) - \frac{1}{2}[(R_2 - R_1)^2 + 4Z_{12}Z_{21}]^{1/2}, \quad (9)$$

$$\Gamma'_m = \frac{1}{2}(R_1 + R_2) + \frac{1}{2}[(R_2 - R_1)^2 + 4Z_{12}Z_{21}]^{1/2}. \quad (10)$$

Γ_m represents the long-lived component and Γ'_m the short-lived component of the atomic decay. The

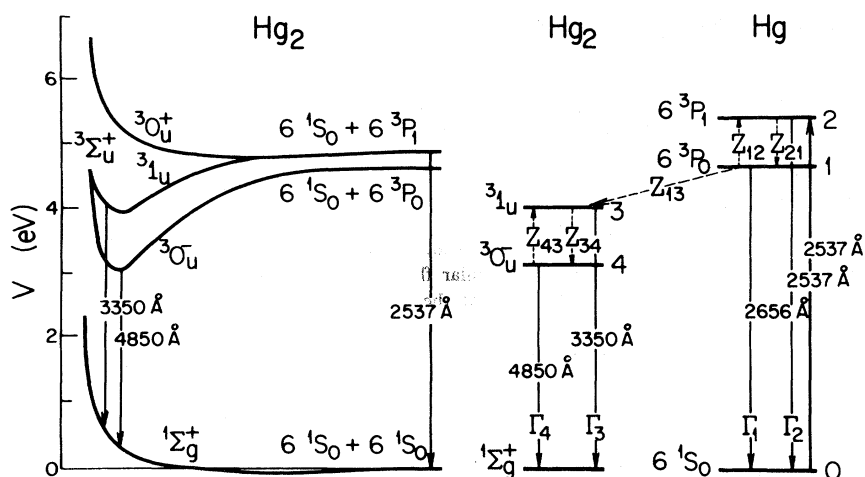


FIG. 1. Schematic diagram of atomic and molecular levels and radiative and collisional processes involved in the sensitized fluorescence of Hg₂ molecules. The molecular potential-energy curves are drawn according to Mrozowski (Ref. 3).

lowest possible value of Γ'_m , which arises at very low mercury vapor pressures, corresponds to the "natural" lifetime of the 3P_1 state⁹ and, consequently, when the atomic decays are observed at very low Hg densities, only the long-lived component Γ_m is observed.¹

However, at high mercury densities, as in the present case, the atomic resonance radiation is trapped, the magnitudes Γ_m and Γ'_m approach each other so that both components can be detected and, consequently, the 3P_0 atoms will decay with two time constants Γ_m and Γ'_m as given by Eq. (7). Similarly, the decay of the 2537-Å afterglow will also contain both Γ_m and Γ'_m , as indicated by Eq. (8). However, since pressure broadening of the Hg 2537-Å absorption line reduces the imprisonment time,¹⁰ the Γ'_m increases in magnitude with increasing argon pressure, and its contribution to the observed decay decreases as it disappears from the region of observation.

Equations (3) and (4) in conjunction with Eq. (7) yield the populations of the Hg₂ excimer states. The resulting inhomogeneous differential equations are

$$\ddot{n}_3 + (R_3 + R_4)\dot{n}_3 + (R_3 R_4 - Z_{34} Z_{43})n_3 = Z_{13} Z_{34} A e^{-\Gamma_m t} + Z_{13} Z_{34} B e^{-\Gamma'_m t}, \quad (11)$$

$$\ddot{n}_4 + (R_3 + R_4)\dot{n}_4 + (R_3 R_4 - Z_{34} Z_{43})n_4 = Z_{13} A (R_4 - \Gamma_m) e^{-\Gamma_m t} + Z_{13} B (R_4 - \Gamma'_m) e^{-\Gamma'_m t}, \quad (12)$$

where $R_3 \equiv \Gamma_3 + Z_{34}$ and $R_4 \equiv \Gamma_4 + Z_{43}$. The general solutions are

$$n_3 = \alpha e^{-\Gamma_b t} + \beta e^{-\Gamma'_b t} + \delta e^{-\Gamma_m t} + \gamma e^{-\Gamma'_m t}, \quad (13)$$

$$n_4 = \alpha' e^{-\Gamma_b t} + \beta' e^{-\Gamma'_b t} + \delta' e^{-\Gamma_m t} + \gamma' e^{-\Gamma'_m t}, \quad (14)$$

where

$$\Gamma_b = \frac{1}{2}(R_3 + R_4) - \frac{1}{2}[(R_3 - R_4)^2 + 4Z_{34} Z_{43}]^{1/2}, \quad (15)$$

$$\Gamma'_b = \frac{1}{2}(R_3 + R_4) + \frac{1}{2}[(R_3 - R_4)^2 + 4Z_{34} Z_{43}]^{1/2}. \quad (16)$$

Γ_b represents the long-lived component and Γ'_b the short-lived component of the molecular decay. The solutions predict that the 31_u and $^30_u^-$ states should decay with the same time constants. The short-lived component Γ'_b is at least as large as Γ_3 which is of the order of 10^7 sec^{-1} . Consequently, no contribution to the decay from Γ'_b can be detected¹ in the range of observation times employed here, and the populations of the molecular states are effectively represented by the expressions

$$n_3 = \alpha e^{-\Gamma_b t} + \delta e^{-\Gamma_m t} + \gamma e^{-\Gamma'_m t}, \quad (17)$$

$$n_4 = \alpha' e^{-\Gamma_b t} + \delta' e^{-\Gamma_m t} + \gamma' e^{-\Gamma'_m t}. \quad (18)$$

II. EXPERIMENTAL

The apparatus used in this investigation has been described elsewhere.¹ Mixtures of mercury vapor and argon, contained in a quartz fluorescence cell at a constant temperature, were irradiated with pulses of mercury resonance radiation emitted by a radiofrequency electrodeless discharge lamp. The resulting fluorescence, emitted at right angles to the direction of excitation, was resolved using appropriate filters followed by a scanning spectrometer, and was detected with a liquid-nitrogen-cooled Philips 56 TUV photomultiplier. The output pulses of the photomultiplier provided the "strobe" signal for the time-to-amplitude converter (TAC), whose "start" signal was generated by a reference photomultiplier, whose photocathode detected a fraction of each exciting light pulse. The use of the "strobe" input in the "external" mode of the TAC, increased the rate of data collection because an output signal resulted from each fluorescent photon reaching the photomultiplier, rather than from just the first photon

following the exciting light pulse. The decay spectrum was accumulated in a 400-channel pulse-height analyzer (MCA) and was recorded on punched paper tape.

The rectangular light pulses which could be produced at different repetition rates, had a duration of 750 μsec , and rise and fall times of about 40 μsec at a repetition rate of 200 pulses/sec. In order to enhance the fluorescent intensities, no filter was used in the exciting light beam. It had been found previously that the absence of a filter does not affect the measured values of the decay constants.¹ The decay spectra which were exponential in character, were analyzed with the aid of an IBM 360-65 computer, using a modified FRANTIC program.¹¹ The modifications made on the TAC, which permitted the use of the "strobe" mode, rendered superfluous the corrections for discrimination against the detection of longer lifetimes.

III. RESULTS AND DISCUSSION

To ensure adequate intensities of the two molecular fluorescence bands, the temperature of the mercury reservoir connected to the fluorescence cell was kept during all the experiments at $(120 \pm 0.2)^\circ\text{C}$, which corresponded to a saturated mercury vapor density of $1.9 \times 10^{16} \text{ cm}^{-3}$; the cell was kept at 194°C , which corresponded to a relative velocity ($\text{Hg}_2\text{-Ar}$) of 520 m/sec.

It had been found elsewhere¹² that the peak of the 4850- \AA band is actually located at 5100 \AA , though the 3350- \AA band peak is at 3350 \AA . These observations tend to agree with those made in the course of this investigation and, consequently, when recording the persistence times of the bands, the spectrometer was set at either 5000 or 3350 \AA . Slits of 2 mm width were used throughout the experiments, which corresponded to a half-band width of about 68 \AA . The decay spectra were obtained at various argon pressures in the range 45–720 Torr. To avoid contamination of the walls, the cell was first baked for several hours, and all experimental runs were begun at a high argon pressure which was then gradually reduced to lower values in the course of the run. Each run was started at a somewhat different argon pressure so that the reproducibility of the data could be verified.

As expected, the two fluorescence bands were found to decay with a common persistence time, a phenomenon which was also observed in the $\text{Hg}_2\text{-Hg}^{13,14}$ and $\text{Hg}_2\text{-N}_2^1$ systems. The presence in the decay of a short-lived negative component which had also been observed in the $\text{Hg}_2\text{-Hg}$ and $\text{Hg}_2\text{-N}_2$ systems^{14,1} and which corresponds to the

decay constant for 2537- \AA afterglow,¹ could be detected only at low argon pressures. It was extracted from the observed decay spectra and separated from the long-lived molecular component Γ_b by computer analysis.¹¹ In the range of observation times that were used, Γ_b was found to contribute most to the over-all decay. Considering that the energy transfer between $\text{Hg } 6^3P_1$ and 6^3P_0 states induced in Hg-Ar collisions is very inefficient,¹⁵ the main contribution to the amplitudes of the second and third exponential terms in Eq. (17) must come from Hg-Hg collisions. However, at low argon pressures, the relative contribution of the short-lived atomic component represented by the third term of Eq. (17) was found to predominate over the contribution of the second term. The fact that the negative component could be separated only at low argon pressures, disappearing as argon pressure was increased, is thought to be directly due to the effect of $\text{Hg } 2537\text{-}\text{\AA}$ line broadening on radiation trapping, and to imply that Γ'_m rather than Γ_m is the predominant ingredient of the negative component in the decay of the molecular fluorescence. This conclusion is quite reasonable if it is considered that the long-lived 2537- \AA afterglow arises directly as the result of $^3P_1 - ^3P_0$ mixing induced in Hg-Ar collisions which have a vanishingly small cross section.¹⁵ This was borne out during attempts to observe the behavior of Γ_m and Γ'_m by monitoring the decay of the 2537- \AA afterglow in relation to argon pressure. The observed number of afterglow photons was very small and consequently, no meaningful conclusions could be reached. Complications arose also from the fact that at low argon pressures, effects due to diffusion of excited atoms could no longer be neglected.

Figure 2 shows the variation of the decay constant Γ_b with argon pressure. Each experimental point represents an average of the decay constants obtained from the two bands at the particular argon pressure and the curve represents a least-squares fit of the experimental data to Eq. (15). In the analysis, Γ_3 was taken as equal to the "natural" spontaneous decay constant of the atomic $\text{Hg}(6^3P_1)$ state ($8.54 \times 10^6 \text{ sec}^{-1}$),¹⁶ and Γ_4 (for the $^3O_u^-$ state) was put equal to the most reliable value obtained by Skonieczny and Krause (46.6 sec^{-1}).⁶ The least-squares analysis yielded the collision numbers Z_{34} and Z_{43} , which are given in Table I together with their standard deviations, and which were used to obtain the corresponding total inelastic cross sections $Q_{34}(^31_u \rightarrow ^30_u^-)$ and $Q_{43}(^30_u^- \rightarrow ^31_u)$, which are also listed in Table I.

Before carrying out the least-squares analysis, it was necessary to assess the influence of dif-

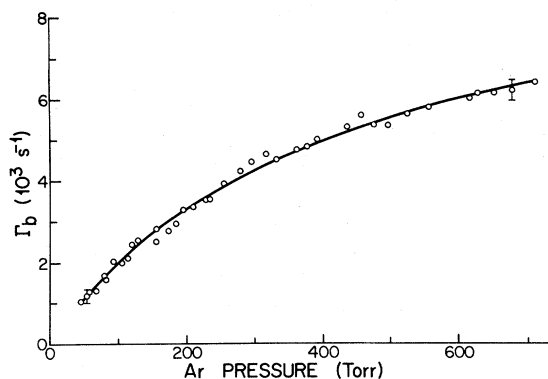


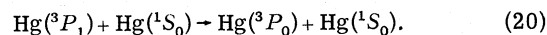
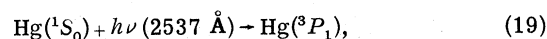
FIG. 2. Variation of the decay constant Γ_b with argon pressure at a mercury vapor density of $1.88 \times 10^{16} \text{ cm}^{-3}$. The two error bars are representative of all the points.

fusion of metastable species out of the region of observation⁷ and to the cell walls.⁸ Additional experimental data, obtained at low argon pressures, are shown in Fig. 3. A least-squares fit of Eq. (15), to all the experimental points, was carried out with the inclusion of an additional term $\Gamma_d = k_1 \exp(-P/k_2)$, which should represent the effect of diffusion on the measured value of Γ_b at an argon pressure P . Figure 3 also includes separate plots of Eq. (15) and of the term Γ_d . It was found that the best fit corresponded to $k_1 = (520 \pm 75) \text{ sec}^{-1}$ and $k_2 = (25 \pm 7) \text{ Torr}$ and that diffusion of metastable species has negligible influence on the data obtained at pressures above 45 Torr, thus requiring no corrections to be applied to the experimental results.

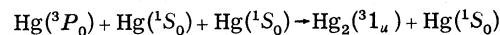
Some additional information about the origins of the molecular fluorescence is provided by intensity measurements on the two molecular fluorescence bands, which were performed in relation to argon density. A plot of $R = I(4850 \text{ \AA})/I(3350 \text{ \AA})$ against argon density is shown in Fig. 4. In the range of 0–100 Torr, the intensity ratio R increases as $(N_{\text{Ar}})^{1/2}$, and it tends to saturate at about 500 Torr. Some additional preliminary measurements of this intensity ratio in relation to Hg density have shown that, at relatively low mercury densities [$(2-4) \times 10^{16} \text{ cm}^{-3}$], the ratio varies as $(N_{\text{Hg}})^{1-6}$, which is in good agreement with the observations of Matland and McCoubrey¹⁷ who worked in the same pressure region, but carried out intensity measurement in the after-

glow rather than using continuous excitation as was done in the present case. At Hg densities above 10^{17} cm^{-3} and temperatures above 575 °K, Drullinger *et al.*¹² found this dependence to be linear and interpreted it as an indication that Hg₃^{*} trimers might constitute the source of the molecular band fluorescence at higher mercury densities.

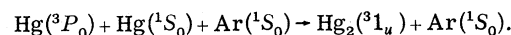
The fact that both molecular fluorescence bands decay with a common persistence time confirms the hypothesis of a common reservoir of excitation energy, which populates both molecular excimer states. There is extensive evidence that this energy reservoir is provided by the atomic metastable Hg(6^3P_0) state.^{1,4,14} This mechanism is based on Mrozowski's early proposals and potential-energy curves for the Hg₂ molecule^{2,3} shown in Fig. 1. The 31_u and $^30_u^-$ excimer states are believed to be formed in the following sequence of processes:



A 3P_0 metastable mercury atom can combine with a ground-state atom, and the pair can become stabilized in a subsequent collision with a ground-state mercury or argon atom:



or (21)



According to Mrozowski's original suggestion² which has also been adopted by subsequent investigators,^{4,5} the 31_u state is the precursor of the $^30_u^-$ state. The two excimer states merge into a single $^3\Sigma_u^+$ state at moderate internuclear distances and in a region which is below the dissociation limit of the $^30_u^-$ state. Consequently, the two states should become populated equally by the reaction $\text{Hg}(^3P_0) + \text{Hg}(^1S_0)$, but collisional stabilization should favor the 31_u state, since no dissociation is possible along the 31_u potential curve. The molecular fluorescence bands are emitted as the result of the following processes:

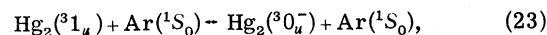
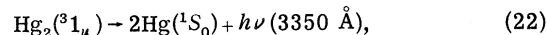


TABLE I. Collisional parameters obtained by least-squares analysis and cross sections for the $^31_u \leftrightarrow ^30_u^-$ mixing (N denotes Ar density).

Z_{34} ($10^{-13}N \text{ sec}^{-1}$)	Q_{34} (10^{-18} cm^2)	Z_{43} ($10^{-16}N \text{ sec}^{-1}$)	Q_{43} (10^{-21} cm^2)	S. D. in Γ_b (sec^{-1})
9.77 ± 0.41	18.7 ± 0.8	11.69 ± 0.24	22.4 ± 0.5	131

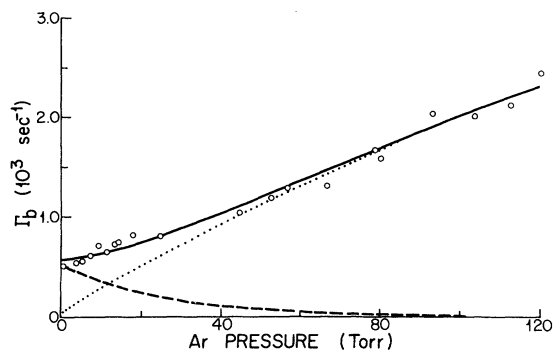
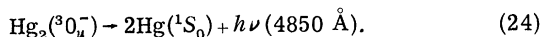


FIG. 3. Variation of the decay constant Γ_b with argon pressure in the low pressure region. The circles represent experimental points; the dotted line represents a plot of Eq. (15); the dashed line represents $\Gamma_d = k_1 \exp(-P/k_2)$; the solid line represents the result of adding the two other curves.



The process represented by Eq. (23) is also efficiently induced in collisions with ground-state mercury atoms. Since the $^3O_u^-$ metastable molecules are able to radiate only when the Hg-Hg internuclear distance is very small,¹ the 4850-Å band is emitted mostly by molecules with high vibrational energies. While the transition probability for $^3O_u^-$ state is variable, increasing with decreasing internuclear distance, a constant transition probability should be expected for the $^3^1_u$ state, comparable to that for the atomic 3P_1 state.

The effective cross sections Q_{34} and Q_{43} for

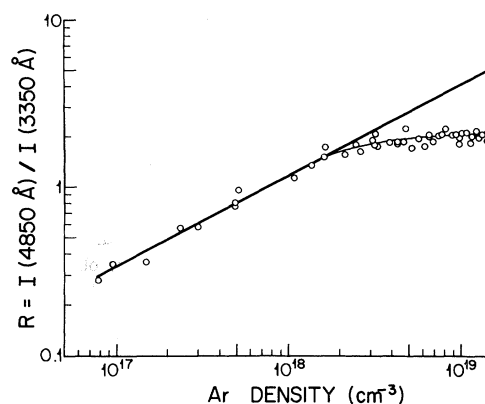


FIG. 4. Variation of fluorescence band intensity ratio $R = I(4850 \text{ \AA}) / I(3350 \text{ \AA})$ with argon density.

$^3^1_u \leftrightarrow ^3O_u^-$ mixing induced in the Hg_2 -Ar collisions are of the same magnitude as the corresponding cross sections for Hg_2 - N_2 collisions.^{1,6} If the general mechanism of formation and decay of the two mercury excimers is correct, then it seems that even in the case of $^3^1_u \leftrightarrow ^3O_u^-$ transfer induced in collisions with N_2 molecules, most of the energy defect between the two states is supplied from or taken up by the translational continuum without involving the molecular vibrational and rotational modes to any large extent. This implies that the energy transfer is virtually resonant and occurs close to the intersection of the two molecular curves, where the energy defect between the two states is very small and the transition probability for the decay of the $^3O_u^-$ excimer is highest.

*Research supported by the National Research Council of Canada.

¹R. A. Phaneuf, J. Skonieczny, and L. Krause, *Phys. Rev. A* **8**, 2980 (1973).

²S. Mrozowski, *Z. Phys.* **106**, 458 (1937).

³S. Mrozowski, *Rev. Mod. Phys.* **16**, 153 (1944).

⁴S. Penzes, H. E. Gunning, and O. P. Strausz, *J. Chem. Phys.* **47**, 4869 (1967).

⁵J. E. McAlduff, D. P. Drysdale, and D. J. LeRoy, *Can. J. Chem.* **46**, 199 (1968).

⁶J. Skonieczny and L. Krause, *Phys. Rev. A* **9**, 1612 (1974).

⁷P. B. Sackett, *Appl. Opt.* **11**, 2181 (1972).

⁸F. A. Franz, *Phys. Rev. A* **6**, 1921 (1972).

⁹J. Pitre, K. Hammond, and L. Krause, *Phys. Rev. A* **6**, 2101 (1972).

¹⁰T. Holstein, D. Alpert, and A. O. McCoubrey, *Phys. Rev.* **85**, 985 (1952).

¹¹P. C. Rogers, FRANTIC, program for analysis of exponential growth and decay curves, MIT Laboratory of Nuclear Sciences, Technical Report No. 76, 1962 (unpublished).

¹²R. E. Drullinger, M. M. Hessel, and E. W. Smith (private communication).

¹³Lord Rayleigh, *Proc. R. Soc. Lond.* **A114**, 620 (1927).

¹⁴A. O. McCoubrey, *Phys. Rev.* **93**, 1249 (1954).

¹⁵J. S. Deech, J. Pitre, and L. Krause, *Can. J. Phys.* **49**, 1976 (1971).

¹⁶J. S. Deech and W. E. Baylis, *Can. J. Phys.* **49**, 20 (1971).

¹⁷C. G. Matland and A. O. McCoubrey (unpublished), quoted in Ref. 12.